

Obstacle Avoidance Behavior for a Biologically-inspired Mobile Robot Using Binaural Ultrasonic Sensors

William A. Lewinger

Department of Electrical Engineering
and Computer Science
Case Western Reserve University
Cleveland, OH, USA
wal4@case.edu

Michael S. Watson

Department of Mechanical and
Aerospace Engineering
Case Western Reserve University
Cleveland, OH, USA
msw14@case.edu

Roger D. Quinn

Department of Mechanical and
Aerospace Engineering
Case Western Reserve University
Cleveland, OH, USA
rdq@case.edu

Abstract – Many untethered mobile robots require an operator’s vision and intelligence for guidance and navigation. Animals and insects, however, use sensory systems such as hearing, and tactile inputs to move autonomously through their environment. This paper discusses the implementation of a binaural sensory pod using an ultrasonic emitter and two receivers on a mobile robot that employs legged-style locomotion. A series of obstacle avoidance behaviors programmed onto a microcontroller allows the robot is to successfully navigate a cluttered environment both semi-autonomously and autonomously.

Index Terms - Obstacle Avoidance, Autonomous Behavior, Non-contact Sensing, Biologically-inspired, Whegs™.

I. INTRODUCTION

Antennae are responsible for much of the orientation behavior exhibited by cockroaches and other insects when they move on the ground. This tactile orientation behavior can be used for wall following [5], identification of a predator [7], and object guided orientation [17]. Antennae may also be used for navigation in complex environments.

Inspired by insects and other animals, robots have been designed with physical antennae and tactile sensors to navigate their environment, as in the work by Brooks [4], Hartmann [9], and the sagittal plane work by Lewinger et al. [13]. While insects have compliant, articulated antennae to sense their environment, mechanical antennae for mobile robots are usually less compliant and can possibly impede the robot while it is navigating difficult terrain. The use of non-contact sensors based on biological hearing can alleviate this problem.

Insects such as crickets [11][14] and small animals like the small brown bat [10][20] have binaural hearing that relies on intensity, or level differences in the sounds received by each hearing sensor. Intensity measurement is used since the separation of the hearing organs is very small. Larger animals like owls [6] and people [15] measure the time delay between the signals received in each ear to determine azimuth. The sound stimuli are compared from each ear to locate the azimuth of the source.

Inspired by the interaural time difference (ITD) method of sound location, as used by larger animals, and using a self-generated sound pulse, as in the echo location of bats

[10][20], a binaural sensor pod was created using ultrasonic sensors. The sensor pod (Fig. 1) consists of a single, centrally-located ultrasonic emitter and two ultrasonic receivers angled outward at 22.5 degrees from the frontal plane.

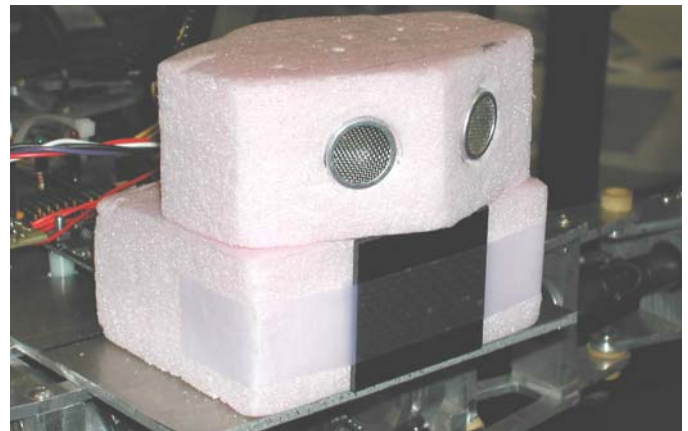


Fig. 1 Binaural ultrasonic sensor pod with single ultrasonic emitter (located behind the black square) and angled dual receivers above.

Using a central emitter eliminated the possibility of conflicting echo signals, which could occur if two emitters were used. Having two receivers separated by a distance allows detected objects to be located in a planar environment by determining the distance between the object and each sensor [8][12]. By angling the wide-field receivers outward two overlapping reception fields were created [2][3]. This allowed fewer receivers to detect the same object and locate its position, rather than using many more narrow-field receivers.

The binaural ultrasonic sensor pod was mounted to the front of a Whegs™ II mobile robot (Fig. 1) that uses a walking-style mode of locomotion abstracted from cockroaches. Using this robot for the sensor platform allowed larger objects to be sensed and avoided and smaller objects to be climbed over; something that wheeled robots of the same size cannot do.

Two obstacle detection and avoidance behaviors were created to locate objects and navigate away from them. The first behavior allowed semi-autonomous operation of the robot

and used a simple method of detecting objects within one of three zones: left, center, and right. Objects sensed in the left or right zones caused the robot to steer away in the opposite direction. Centrally-located obstacles stopped the robot's forward progress and required an operator to reverse direction and choose a new heading.

The second behavior provided the robot will full autonomy. It used a 2m sensor range and determined the azimuth of obstacles using interaural time differences. Once the location of an object was calculated, steering and drive speed were adjusted proportionately based on position and distance of the object.

II. WHEGS™ II FEATURES

The patented Whegs™ II (Fig. 2) uses a single 90W Maxon DC motor to propel all six of its legs. The single propulsion motor design reduces the robot's weight and improves its power to weight ratio [1][18]. Its three-spoke wheel-leg appendages, abstract the principles of a cockroach's leg cycle while rotating at constant speed. This configuration permits the leg to get a foothold on an obstacle that is higher than the length of a spoke.

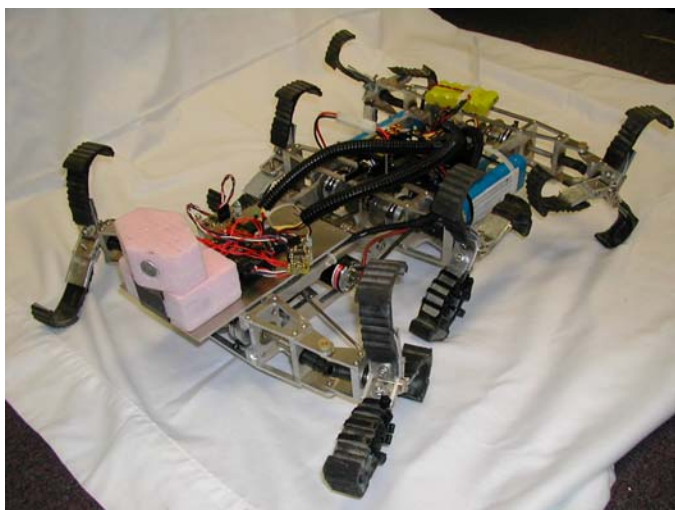


Fig. 2 Whegs™ II mobile robot with binaural ultrasonic sensor pod mounted on the front.

The simplified legs are installed on the vehicles such that they form a nominal tripod gait [21]. Torsional compliant mechanisms at each wheel-leg permit the robot to passively adapt its gait to the terrain. Whegs™ II uses 10cm long spokes that move in the sagittal plane (Fig. 2). Whegs™ II is steered by two small R/C servos that are electrically coupled to rotate the front and rear legs in opposite directions.. The body and geometry of Whegs™ II gives it a turning radius of 1.25 body lengths.

Robots with spoke legs preceded Whegs™. The PROLERO hexapod robot used a single rotating spoke design for each of its six legs. It used six motors, one for each leg, to rotate its legs in a circular motion to enable walking and turning [16]. RHex expanded upon this single spoke concept

by incorporating compliant legs and a more complex control architecture [19].

III. ULTRASONIC SENSOR CHARACTERISTICS

Devantech SRF08 ultrasonic range-finding units (Devantech Ltd., Norfolk, UK) were used as the basis for the sensor pod and have a single emitter and a single receiver mounted to a small board containing signal processing electronics. They were chosen for their balance of accuracy, range, speed, and cost.

While there is available information on the SRF08, experiments were conducted to determine the actual range capabilities and the sensor envelope. These measurements were required to fully characterize the sensors before integrating two of them into the sensor pod.

The first set of experiments was performed to determine the sensor envelope of a single, unmodified SRF08. Two sets of planar tests were performed to calculate a three-dimensional representation of the envelope. Each of the planar tests had the Devantech SRF08 firmly mounted 1.2m from the floor. The first test had the sensor mounted so that the emitter and receiver were positioned side-by-side. The second test had the sensing elements positioned one above the other. These tests were designed to determine the xy-plane envelope and the yz-plane envelope.

To find the sensor envelope, a 120cm long, 15cm diameter tube was placed at various locations in front of the SRF08. At each location the Devantech sensor was queried whether it could detect the tube or not. Initially, the tube was moved at 30cm increments to grossly determine the envelope. Then, smaller movement increments were used to get a more accurate image of the sensing ranges and angles. Points at which the SRF08 was able to detect the tube were plotted to define the boundary of the sensor envelope (Fig. 3, top).

The Devantech SRF08 detected the tube at distances up to 7.6m. The initial sensing field was an arc of approximately 90 degrees for a distance of about 3m. Beyond 3m the envelope maintained a fixed width of about 8m. Tests performed with the sensor mounted vertically showed similar results, indicating a conical sensor envelope. Other experiments were performed with tubes of smaller diameters down to 5cm. The SRF08 was able to detect the smaller object throughout the entire envelope.

After the envelope was determined for the single, unmodified Devantech SRF08 ultrasonic sensor, the sensors were altered for use as a binaural set. The emitter and receiver were unsoldered from the electronics board and re-connected to the board by 15cm long cables. This allowed the emitter and receiver to be mounted at new angles relative to one another. The emitter and receiver from a single SRF08 were used as the central emitter and right receiver. A second SRF08 was similarly modified and formed the left receiver. Since the emitter is integral to the circuitry of the SRF08 the second emitter remained attached to the electronics board but was shielded so that it didn't create additional echoes.

Once modified, the emitter and two receivers were mounted in foam (Fig. 1). The receivers were separated by 35mm and angled 22.5 degrees from the frontal plane. The emitter was centrally located, 50mm below the receivers.

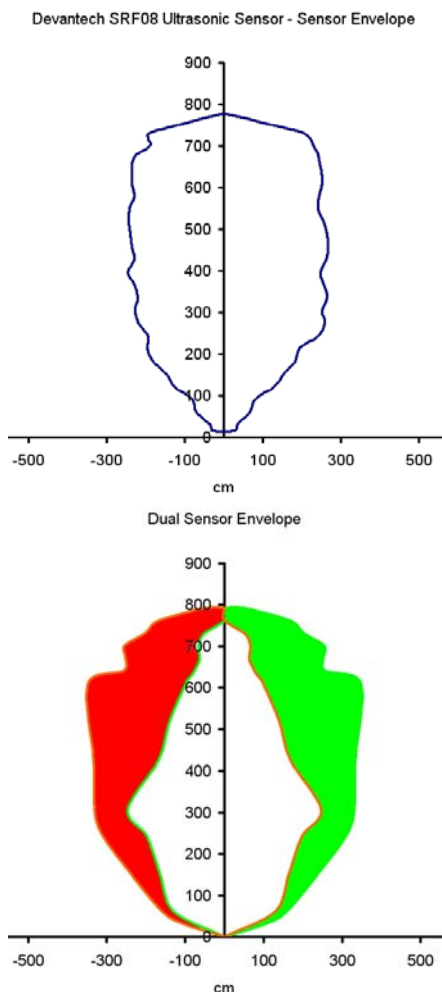


Fig. 3 Sensor envelope for a single Devantech SRF08 (top), and sensor envelope for the binaural ultrasonic sensor pod with a single emitter with angled dual receivers (bottom).

Additional experiments were then performed to determine the new xy-plane sensor envelope for the binaural ultrasonic sensor pod. The new experiments were conducted in a similar manner with a 120cm long, 15cm diameter tube at various positions in front of the sensor pod. The left and right sensor envelopes mirrored one another and expanded the detection angle near the pod from 90 degrees to about 105 degrees (Fig. 3, bottom) for a distance of about 3m. Beyond 3m the combined envelope detected objects in a 7m wide path out to a range of about 8m.

While the receivers are capable of detecting echoes from angles of ± 45 degrees, the emitter cannot send ultrasonic pulses over a range of 135 degrees (the full possible sensory range of two receivers angled 45 degrees apart). As a result, the sensor envelope for the binaural sensor pod is limited to 105 degrees.

By using two receivers at a splayed angle, three sensory zones were created. There are two outer zones where only a single sensor can detect an object (colored areas of Fig. 3, bottom), and a central zone where both sensors receive echoes from the same target (white area of Fig. 3, bottom).

Using a single emitter with a pair of receivers widens the sensor envelope, improves detection performance, and reduces sensing time. Activating two emitter/receiver pairs at the same time would cause spurious echoes that would confuse the sensors. To eliminate this possibility, each sensor pair would need to emit and receive echoes before activating the other sensor pair. This would double the time required for both sensors to detect objects. A single emitter with two receivers eliminates the echo interference and long detection time issues.

IV. IMPLEMENTATION AND BEHAVIOR

The binaural ultrasonic sensor pod (described above) was mounted to the front of the Whegs™ II chassis where it had an unobstructed view of the area ahead of the robot (Fig. 2). This mounting placed the emitter approximately 15cm from the ground with the receivers 20cm from the ground.

Initially, ground reflections were observed approximately 15cm in front of the robot. Attempts to remedy the situation included additional shielding between the ultrasonic emitter and receivers in the form of a horizontal plate of carbon fiber. This, however, was insufficient. In the end, a carbon fiber filter was placed over the emitter (the black square in Fig. 1) to attenuate the broadcasted signal. This reduced the intensity of the emitter signal and allowed the sensors to ignore almost all ground reflections.

An Acroname BrainStem microcontroller (Acroname, Boulder, CO, USA) was mounted behind the sensor pod and was used to trigger the ultrasonic emitter and read echo signals from each of the receivers.

The ultrasonic range-finders continuously reported the distance of the first echo every 100msec. This time was chosen to be larger than the maximum 65msec timeout value representing the farthest distance the range-finders could detect objects (11m).

Two separate behaviors were programmed into the robot. The first was used in a semi-autonomous mode where an operator drove the robot and the binaural sensor pod detected obstacles and corrected the robot's course and/or speed, overriding the operator's commands. The second was fully autonomous operation where the robot determined its own steering angle and drive speed based on the location and distance of detected obstacles without any input from an operator.

For semi-autonomous operation the BrainStem also interpreted radio control commands from the R/C receiver as initiated by the operator. The three R/C channels that control speed, steering, and the body flexion joint were all interpreted by the BrainStem and then modified, as needed, based on the detection of sensed obstacles.

The R/C channel signals were interpreted by reading the pulse width (0.9msec – 2.1msec) from the R/C receiver with the level transition detecting capabilities of the BrainStem digital I/O ports. The pulse width was converted to an 8-bit value with 0.9msec corresponding to 0 and 2.1msec corresponding to 255. This represented the full range of R/C servo values that could be sent out to the Whegs™ II steering and body joint motors and the drive motor speed controller to actuate and move the robot. When no obstacles were detected in the path of the robot, the operator commands were passed on to the robot motors without modification.

During semi-autonomous mode (1) an obstacle warning distance of 75cm was set as a software threshold for when the avoidance behavior would take action. If an obstacle appeared in the left field, the robot would turn to the right to avoid a collision. This was accomplished by replacing the operator's intended steering control value and creating a full-right turn signal to be sent to the steering servo motors instead. The operator's intended signal was still interpreted by the BrainStem, but then ignored in favor of the behavior's control signal. Once the object was no longer detected within range, the operator's signal was once again sent to the steering servo motors. Similarly, obstacles appearing in the right field would cause the robot to steer to the left until the obstacle was no longer detected.

$$threshold = 75cm$$

```

if (left sensor < threshold and right sensor > threshold)
  turn full right
if (left sensor > threshold and right sensor < threshold)
  turn full left
if (left sensor < threshold and right sensor < threshold)
  stop forward motion
  
```

(1)

This avoidance behavior created the ability for the robot to follow a wall. If the operator drove the robot forward while steering it toward a wall, the robot would approach the wall until a potential collision was detected. Then, the obstacle avoidance behavior would steer the robot away from the wall while it still moved forward. When the wall was no longer in range, the operator's steering command would resume and the robot would once again head toward the wall.

If both left and right ultrasonic receivers detected an obstacle, indicating the presence of something in the center field, forward motion was stopped. In this case the operator could fully steer the robot between the left and right extremes, but could only drive in reverse.

While the threshold distance was set to 75cm, the actual distance at which actions were taken varied with the angle the obstacle face had with the mid-sagittal plane. The more acute the angle, the closer the robot came to the obstacle before an autonomous action was taken. In two cases, the angle of the wall with the mid-sagittal plane was very small (less than 15 degrees) and glancing impacts occurred.

For the second, fully autonomous behavior (2) a sensory threshold of 2m was set. Objects beyond 2m were ignored.. Obstacles within 2m were still considered to be in one of the three detection zones: left, center, and right.

When an obstacle was detected three calculations were made: average range to the target for both receivers (rangeAvg), an effective distance by which obstacle avoidance intensity was determined (rangeDist), and a difference in distance values sensed by the two receivers (rangeDiff).

If a detected obstacle is sensed by both receivers and the difference in the measured distances is less than the distance between the two sensors, both receivers are detecting the same object. In this case, steering is inversely proportional to the distance of the object or its location to the side of the robot's path. For example, objects that are far away or to the side of the robot create a smaller steering angle from the current path.

$$sensing\ threshold\ (threshold) = 2000mm$$

$$sensor\ separation\ (separation) = 35mm$$

$$sgn(val) = 1\ if\ val > 0\ else\ -1$$

$$rangeAvg = (right\ sensor + left\ sensor) / 2$$

$$rangeDist = threshold - rangeAvg$$

$$rangeDiff = (right\ sensor - left\ sensor) / separation$$

$$if\ (abs(left\ sensor - right\ sensor) < separation)$$

$$steerVal = 128 + (rangeDist / rangeDiff) * \quad (2)$$

$$sgn(rangeDiff)$$

$$else\ if\ (right\ sensor < left\ sensor)$$

$$steerVal = 128 + (threshold - right\ sensor) / 92$$

$$rangeAvg = right\ sensor$$

$$else\ if\ (right\ sensor < left\ sensor)$$

$$steerVal = 128 + (threshold - right\ sensor) / 92$$

$$rangeAvg = left\ sensor$$

$$driveVal = 128 + (rangeAvg * 128 / threshold)$$

If detected distances differ by more than the distance between the sensors more than one obstacle is detected and the sensor with the closer object has priority. In this case steering is still inversely proportional to the distance to the obstacle, but the difference between the left and right sensors is not taken into consideration.

Speed is proportional to obstacle distance. The farther away an obstacle is located, the faster the robot moves forward. If an object is in front of the robot and it cannot be avoided by steering, forward speed is reduced to zero and the robot stops. The current behavior doesn't allow the robot to drive in reverse.

Once steering and speed values are calculated, the commands are autonomously sent to the steering servo motors and drive motor speed controller.

V. EXPERIMENT SCENARIOS

Experiments for the semi-autonomous behavior were performed in a 1.5m wide, 8.5m long section of hallway. The

floors were covered with 30cm square vinyl tiles. The walls were formed of painted concrete blocks with 10cm tall vinyl strips at the base.

Two series of experiments for this behavior were conducted. The first was a set of wall-following tests. The second was a set of two unique obstacle courses. The obstacle course contained six 60cm tall, 12cm diameter cardboard cylinders placed at random along the length of the course.

For the wall-following scenario, the operator drove the robot forward while steering toward either the left or right wall. In the obstacle course scenario, the operator drove the robot generally forward, allowing autonomous course corrections to avoid collisions. However, some operator steering was used to intentionally choose paths toward obstacles.

Additionally, operator driving and steering was used in the obstacle course scenario when an obstacle was detected in the center field of view. During these cases, the operator controlled the robot to drive in reverse until the obstacle was no longer in range and chose a new heading when resuming forward motion.

For the fully autonomous behavior similar wall-following and obstacle course experiments were performed. These experiments took place in a square room (4.9m long, 3.7m wide) with similar flooring and walls as the semi-autonomous experiments.

Wall-following trials were conducted about the perimeter of the room. For later experiments obstacle courses with three and four 60cm tall, 12cm diameter cardboard cylinders were created. Additional experiments were also performed in both the wall-following and obstacle course scenarios with low (5cm tall) obstacles for the robot to climb over.

Each fully autonomous trial began with placing the robot in the test environment. The robot was then manually activated and no further operator actions were taken until the trial ended and the robot was deactivated. The robot decided its heading and speed through its environment based solely on sensor inputs.

VI. RESULTS

Eight experiments were conducted with the semi-autonomous behavior. Six trials were performed for the wall-following scenario and two trials were performed with the obstacle course scenario. For the second set of trials one run was performed in each of two unique obstacle courses.

One run is shown in Fig. 4, left. The actual path taken by the robot is shown in blue. Short red lines indicate times when the operator directed the robot toward the wall but the obstacle avoidance behavior steered away from the impending collision. Six autonomous course corrections were made by the behavior and no wall collisions occurred. For these trials, 31 of 33 collisions with the wall were avoided (94% success).

Fig. 4, middle and right show semi autonomous runs through obstacle courses. The obstacle avoidance behavior avoided 25 out of 26 collisions (96% success). In the first obstacle course the robot collided with the wall and required

operator action to correct the situation. The obstacle avoidance behavior performed the correct steering action, however, the robot was too close to the wall when it was detected and it was too late to prevent the collision. There were no collisions with walls or other obstacles during the second obstacle course.

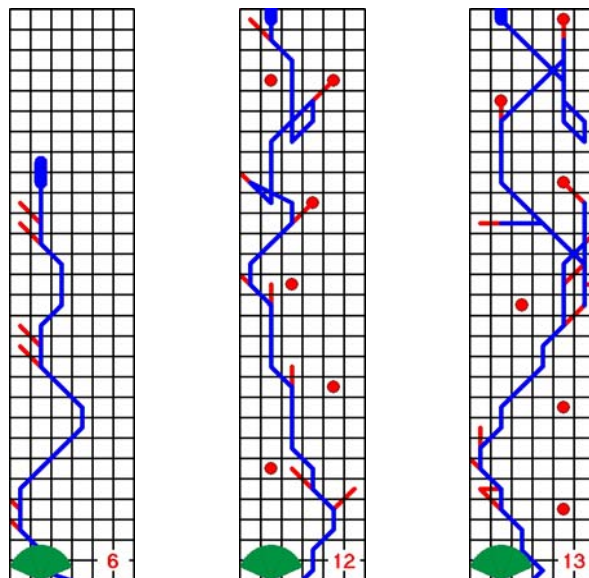


Fig. 4 Robot paths for wall following (left), and two unique obstacle courses (middle and right). Red lines show the commanded path that wasn't chosen. Numbers indicate times that an autonomous course correction was made due to a sensed obstacle. The robot moved from bottom to top in each case.

Forty-five experiments were conducted with the fully autonomous behavior: 32 wall-following trials, and 13 obstacle avoidance trials.

During the wall-following trials the robot was placed near a wall and activated. If the robot was close enough to the wall it approached the wall and steered away such that the angle with the wall became increasingly shallow. Also, as the robot came closer to the wall the speed decreased. The robot continued to follow the wall until it found a corner, at which time it stopped since there was no path it could take according to the programmed behavior. If the robot started farther from a wall it could successfully turn away from an encountered corner and continue about the enclosed room following the perimeter. Throughout these trials no wall collisions occurred.

Five of the wall-following trials involved a low (5cm) obstacle that the robot was easily capable of climbing. During four of these trials, the ultrasonic sensor field detected the low obstacle and considered it impassable, at which time the robot came to a halt. After modifying the sensor field by blocking the lower portion of the sensor envelope, the robot successfully followed the wall while ignoring the presence of the low obstacle, which was easily surmounted. The robot did not collide with wall during any of these trials.

The second series of trials involved six runs through a course with three tall, cylindrical obstacles, four runs through

a course with four tall, cylindrical obstacles, and three runs through the four-obstacle course with an additional low obstacle.

During these trials, as with the wall-following scenario, the robot steered away from obstacles proportionally to their distance in front of the robot and distance away from the robot's path. In a few cases the robot approached an obstacle head-on and was not able to steer away from it. In these cases the robot stopped in front of the obstacle without contacting it.

As with the low obstacle scenario during the wall-following trials the robot initially considered the obstacle something to be avoided and steered away from it. Once the sensor field was modified to ignore low obstacles, the robot successfully climbed over the low obstacle in the other two trials.

It should be noted that during the fully autonomous obstacle course trials, as with the wall-following trials, no collisions with either wall or other obstacles occurred (100% success).

VII. CONCLUSIONS AND FUTURE WORK

While the test areas were uncluttered other than the placed obstacles, there were still opportunities for physical antennae to hinder the robot's mobility or become damaged. These dangerous scenarios were avoided altogether by using binaural ultrasonic sensing instead.

With a 95% success rate for semi-autonomous trials and 100% success during the fully autonomous trials, the binaural ultrasonic sensor pod and programmed avoidance behavior has proven itself useful as a mobile robot navigation aid. By using the modular design implemented for these experiments, the sensor pods could be integrated with other mobile robots to provide non-contact sensing and navigation for them as well.

Future experiments will be performed with modifications to the binaural ultrasonic sensor pod. One alteration will be the permanent alteration of the sensor field. This modification will allow the robot to ignore low obstacles that could be easily climbed over.

The behaviors will also be altered to consider information from both left and right receivers when the sensed distance to objects differs by more than the distance between the sensors. This will allow the robot to both follow a wall on one side, for example, while planning to avoid an oncoming obstacle, thus preventing situations where the robot drives into a corner and stops. By implementing additional path recognition and goal-oriented behaviors, the binaural ultrasonic sensor pod can assist fully autonomous mobile robots with path navigation, not just obstacle avoidance.

REFERENCES

- [1] Allen, T. A., Quinn, R. D., Bachmann, R. J., and Ritzmann, R. E. (2003) "Abstracted Biological Principles Applied with Reduced Actuation Improve Mobility of Legged Vehicles," IEEE International Conference on Intelligent Robots and Systems (IROS 2003), Las Vegas, NV, USA, 2003.
- [2] Bank, D (2002) "A High-Performance Ultrasonic Sensing System for Mobile Robots," In *ROBOTIK 2002: Leistungsstand, Anwendungen, Visionen, Trends. VDI-Berichte Nr. 1679*, Editor: VDI-Verlag. June 2002, pp. 557-564.
- [3] Bank, D. (2002) "A Novel Ultrasonic Sensing System for Autonomous Mobile Systems," *IEEE Sensors Journal*, Vol. 2, No. 6, pp. 597-606, 2002.
- [4] Brooks, R. A. "A Robot that Walks; Emergent Behavior from a Carefully Evolved Network", *Neural Computation*, 1:2, Summer 1989, pp. 253-262. Also in IEEE International Conference on Robotics and Automation, Scottsdale, AZ, May 1989, pp. 292-296.
- [5] Camhi and Johnson (1999) "High frequency steering maneuvers mediated by tactile cues: antennal wall following in the cockroach" *J. exp. biol.* 202(5): 631-643, 1999.
- [6] Carr, C. E. and Konishi, M. (1990) "A Circuit for Detection of Interaural Time Differences in the Brain Stem of the Barn Owl," *The Journal of Neuroscience*, Oct. 1990, 10(10): 3227-3246, 1990.
- [7] Comer CM, Parks L, Halvorsen MB, Breese-Terteling A. (2003) "The antennal system and cockroach evasive behavior. II. Stimulus identification and localization are separable antennal functions". *J. comp. physiol. [A]* 189(2):97-103, 2003.
- [8] Feiten, W., Bauer, R., and Lawitsky, G. (1994) "Robust Obstacle Avoidance in Unknown and Cramped Environments", In *Proceedings of the IEEE International Conference on Robotics and Automation (ICRA)*, pp. 2412-2417, 1994.
- [9] Hartmann, M. J. (2001) "Active sensing capabilities of the rat whisker system", *Autonomous Robots*, 11:249-254.
- [10] Horiuchi, T. and Hynna, K. M., (2001) "Spike-based Modeling of the ILD System in the Echolocating Bat", *Neural Networks (Special issue on Spiking Neurons in Neuroscience and Technology)*, vol. 14, pp. 755-762, 2001.
- [11] Horchler, A. D., Reeve, R. E., Webb, B. H., and Quinn, R. D., (2003) "Robot Phonotaxis in the Wild: a Biologically Inspired Approach to Outdoor Sound Localization," 11th International Conference on Advanced Robotics (ICAR'03) Coimbra, Portugal, June 30-July 3, 2003.
- [12] Lawitsky, G., Feiten, W., and Möller, M. (1995) "Sonar sensing for low-cost indoor mobility," *Robotics and Automation Systems*, Vol. 14, pp. 149-157, 1995.
- [13] Lewinger, W. A., Harley, C. M., Ritzmann, R. E., Branicky, M. S., and Quinn, R. D. (2005) "Insect-like Antennal Sensing for Climbing and Tunneling Behavior in a Biologically-inspired Mobile Robot," IEEE International Conference on Robotics and Automation (ICRA'05) Proceedings, Barcelona, Spain, April 18-22, 2005.
- [14] Lund, H. H., Webb, B., and Hallam, J. (1998) "Physical and temporal scaling considerations in a robot model of cricket calling song preference," *Artificial Life*, 4, 95-107, 1998.
- [15] Martin, K. D. (1995), "Estimating Azimuth and Elevation from Interaural Differences," presented at the 1995 IEEE Mohonk workshop on Applications of Signal Processing to Acoustics and Audio, October 1995.
- [16] Martin-Alvarez, A., De Peuter, W., Hillebrand, J., Putz, P., Matthyssen, A. And De Weerd, J.F. (1996) Walking robots for planetary exploration missions. *Second World Automation Congress (WAC '96)*. Montpellier, France, May 27-30, 1996.
- [17] Okada J. and Toh Y. (2000) "The role of antennal hair plates in object-guided tactile orientation of the cockroach (*Periplaneta americana*)". *J. Comp. Physiol. [A]*, 186(9):849-57, 2000.
- [18] Quinn, R. D., Nelson, G. M., Ritzmann, R. E., Bachmann, R. J., Kingsley, D. A., Offi, J. T. and Allen, T. J. (2003), "Parallel Strategies For Implementing Biological Principles Into Mobile Robots," *Int. Journal of Robotics Research*, 2003.
- [19] Saranlı, U., Buehler, M. and Koditschek, D. (2001). RHex a simple and highly mobile hexapod robot. *Int. J. Robotics Research*, 20(7): 616-631.
- [20] Shi, R., and Horiuchi, T. (2004) "A VLSI model of the bat lateral superior olive for azimuthal echolocation", *Proceedings of the 2004 International Symposium on Circuits and Systems (ISCAS'04)*, May 23-26, 2004.
- [21] Watson, J. T., Ritzmann, R. E. (1998) "Leg Kinematics and Muscle Activity during Treadmill Running in the Cockroach", *Blaberus discoidalis*: I. Slow running," *J. comp. physiology*, Vol. 182: 11-22, 1998.